

See discussions, stats, and author profiles for this publication at: <https://www.researchgate.net/publication/49683699>

Affinity of Four Polar Neurotransmitters for Lipid Bilayer Membranes

ARTICLE *in* THE JOURNAL OF PHYSICAL CHEMISTRY B · JANUARY 2011

Impact Factor: 3.3 · DOI: 10.1021/jp108368w · Source: PubMed

CITATIONS

11

READS

32

6 AUTHORS, INCLUDING:



Fengbin Ye

University of Copenhagen

11 PUBLICATIONS 109 CITATIONS

SEE PROFILE



Peter Westh

Roskilde University

183 PUBLICATIONS 3,442 CITATIONS

SEE PROFILE

Affinity of Four Polar Neurotransmitters for Lipid Bilayer Membranes

Chunhua Wang,^{†,§} Fengbin Ye,[†] Gustavo F. Valardez,^{‡,§} Günther H. Peters,^{‡,§} and Peter Westh^{*,†,§}

Research Unit for Functional Biomaterials, NSM, Roskilde University, 1 Universitetsvej, DK-4000 Roskilde, Denmark, Department of Chemistry, Technical University of Denmark, DK-2800 Lyngby, Denmark, and MEMPHYS—Center for Biomembrane Physics, Department of Physics and Chemistry, University of Southern Denmark, Campusvej 55, DK-5230 Odense M, Denmark

Received: September 2, 2010; Revised Manuscript Received: November 10, 2010

Weak interactions of neurotransmitters and the lipid matrix in the synaptic membrane have been hypothesized to play a role in synaptic transmission of nerve signals, particularly with respect to receptor desensitization (Cantor, R. S. *Biochemistry* **2003**, 42, 11891). The strength of such interactions, however, was not measured, and this is an obvious impediment for further evaluation and understanding of a possible role for desensitization. We have used dialysis equilibrium to directly measure the net affinity of selected neurotransmitters for lipid membranes and analyzed this affinity data with respect to calorimetric measurements and molecular dynamics simulations. We studied an anionic (glutamate), a cationic (acetylcholine), and two zwitterionic (γ -aminobutyric acid and glycine) neurotransmitters, and membranes of pure dimyristoyl phosphatidylcholine (DMPC), DMPC doped with 10% anionic lipid (dimyristoyl phosphatidylglycerol, DMPG, or dimyristoyl phosphatidylserine, DMPS), or 1:1 mixtures of dipalmitoyl phosphatidylcholine (DPPC) and dilauroyl phosphatidylcholine (DLPC). The results showed a remarkable variability among the investigated systems. For example, the chloride salt of acetylcholine interacts unfavorably with DMPC and is thus preferentially excluded from the membrane's hydration layer. Conversely, the zwitterionic neurotransmitters are attracted to membranes with 10% anionic lipid and their local concentration at the interface is 5–10 times larger than in the aqueous bulk. The simulations suggest that this attraction mainly relies on electrostatic interactions of the amino group of the neurotransmitter and the lipid phosphate. We conclude that moderate attraction to lipid membranes occurs for some polar neurotransmitters and hence that one premise for a theory of bilayer-mediated modulation of nerve transmission seems to be fulfilled. However, the strong variability in interaction strengths also shows that this attraction is not an inherent property of all neurotransmitters.

Introduction

Weak interactions of small molecules at membrane interfaces have been proposed to influence a number of physiological processes.^{1–3} Recently, a particularly interesting example of this was suggested by Cantor,⁴ who proposed that neurotransmitters (henceforth abbreviated NTs) might, in addition to their well-known effect through the specific and saturable binding to channels in the postsynaptic membrane, modulate synaptic transmission by their partitioning into the membrane. More specifically, it was hypothesized that diffusion of NTs into the lipid matrix of the postsynaptic membrane might cause a shift in conformational equilibria of the channel proteins and that this in turn could cause neural desensitization.⁴ One fascinating aspect of this hypothesis is that it offers an explanation for the invariance in the sensitivity to anesthetics, which has been documented in a range of animal taxa.^{4,5} This invariance is remarkable inasmuch as many general anesthetics never occur in nature and, consequently, no conspicuous selection pressure toward a constant sensitivity can be identified. If, however, the NTs modulate transmission through weak membrane interactions, the highly conserved effect of anesthetics may rely on their mimicry of this modulation.⁴ This hypothesis has recently

been supported by results from whole-cell electrophysiology, where Milutinovic et al.⁶ showed that ligand gated ion channels were modulated in an “anesthetic-like” fashion by nonnative ligands (i.e., neurotransmitters that were not the natural agonist for the ion channel under study).

Two fundamental biophysical questions, which need to be clarified for a further evaluation of this theory, are (i) what is the net affinity of NTs for lipid membranes (that is, to what extent do the neurotransmitter molecules diffuse into the membrane at equilibrium) and (ii) what is the main orientation and location of transmitter molecules when close to—or inside—the membrane? Among the few studies addressing these questions, Rolandi et al.⁷ used capacitance measurements of so-called black lipid membranes to estimate the interaction of γ -aminobutyric acid (GABA) and phosphatidyl serine (PS) membranes. These workers concluded that the membrane was essentially impenetrable to the NT and also reported that sub-millimolar concentrations of GABA reduced the negative potential at the membrane–water interface. The latter was interpreted as an adsorption of cationic species of (the zwitterionic) GABA to the negative PS surface. Pico et al.^{8,9} have studied the adsorption of amino acids (including some NTs) to membranes from hemolyzed red cells and found that glycine adsorbed to the membranes while glutamate did not. To elucidate the two questions (i) and (ii), we have used dialysis equilibrium measurements to quantify the net affinity of four common NTs for unilamellar vesicles of both pure uncharged,

* To whom correspondence should be addressed. Telephone: +45 4674 2879. Fax: +45 4674 3011. E-mail: pwesth@ruc.dk.

[†] Roskilde University.

[‡] Technical University of Denmark.

[§] University of Southern Denmark.

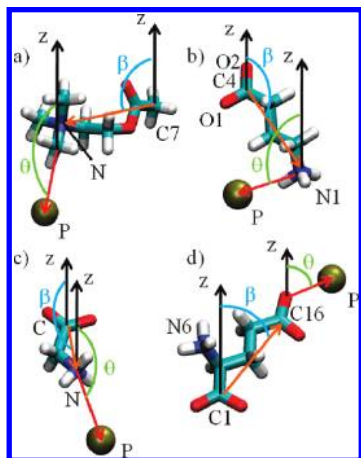


Figure 1. Structures of the neurotransmitters used in the simulations: (a) acetylcholine (ACH; counterion, Cl^-), (b) γ -aminobutyric acid (GABA), (c) glycine (GLY), and (d) glutamate (GLU; counterion, Na^+). Atom types displayed correspond to the protein data bank nomenclature, and these atoms were used for the analysis of the minimum distance between neurotransmitter and phospholipid bilayer ($\text{NT}_{\text{atom}} - \text{P}_{\text{bilayer}}$). θ is the angle between the minimum distance vector (colored red) and the z -axis (perpendicular to the bilayer plane). β is the angle between the head–tail distance vector, d (ACH, $d_{\text{N}-\text{C}7}$; GABA, $d_{\text{N}1-\text{C}4}$; GLY, $d_{\text{N}-\text{C}}$; GLU, $d_{\text{C}16-\text{C}1}$; colored orange), and the z -axis.

mixed uncharged, and mixed anionic lipid membranes. Furthermore, we have used molecular dynamics (MD) simulations to identify the molecular origin of a possible attraction and to elucidate the location and orientation of NTs at a membrane interface.

Methods and Materials

Lipids dimyristoyl phosphatidylcholine (DMPC), dimyristoyl phosphatidylglycerol (DMPG), dimyristoyl phosphatidylserine (DMPS), dipalmitoyl phosphatidylcholine (DPPC), and dilauroyl phosphatidylcholine (DLPC) were purchased as powders from Avanti Polar Lipids (Birmingham, AL). The stated purity was >99%, and the lipids were used without further purification. All samples were extruded into unilamellar liposomes by 10 passages through two stacked 100 nm polycarbonate filters from Nucleopore (Knebel, Denmark) in a Lipex extrusion device (Northern Lipids Inc., Vancouver, BC, Canada). Prior to the extrusion, samples of pure (one-component) lipids were hydrated with Milli-Q water to a lipid concentration of 2–3% (w/w) (all quantifications of suspensions and solutions were done gravimetrically). The lipid suspensions were annealed above the lipid main transition temperature and regularly shaken vigorously over at least 1 h before the extrusion. For mixed (two-component) liposomes, the lipids were initially dissolved in a 2:1 chloroform:methanol solvent. The organic solutions of lipids were subsequently mixed in the appropriate proportions, and excess solvent was driven off in a rotary evaporator at room temperature. Possible traces of the chloroform/methanol mixture were removed by an overnight exposure to vacuum (ca. 0.1 mbar) at room temperature. The dried lipid was then hydrated and extruded in the same way as the one-component samples.

Neurotransmitters of the highest available purity were purchased from different sources. Acetylcholine (chloride salt, abbreviated AChCl) and γ -aminobutyric acid (GABA) were from Sigma (St. Louis, MO), monosodium glutamate (NaGLU) was from Fluka (Buchs, Switzerland), and Glycine (GLY) was from Merck (Darmstadt, Germany). The structures of the NTs are shown in Figure 1.

The affinity of the NTs for unilamellar liposomes of different composition was assessed by dialysis equilibrium measurements. About 0.5 mL of lipid suspension (~2% w/w) was transferred to a dialysis bag from Spectrum Laboratories Inc. (Breda, The Netherlands) with 12–14 kDa molecular weight cutoff. The bag was floated in an ~200 mL solution of one of the NTs in a closed glass beaker placed on a shaking table, which was housed in a thermostated box (air bath). The experimental strategy was then to use ultra performance liquid chromatography (UPLC; see below) to measure concentration differences across the dialysis membrane after the concentration of the NT had been equilibrated over both the dialysis and the lipid membranes. To evaluate the time required to attain equilibrium across the dialysis membrane, we conducted control experiments with pure water in the dialysis bags, and found that the gradient in NT concentration was below the UPLC resolution level (~0.05 mM) in less than 16 h. Based on this, a dialysis time of ~24 h was chosen for all subsequent trials. The permeability of polar NTs through lipid bilayers is very low,⁹ but temperature scanning through the main (gel-to-fluid) phase transition is associated with massive membrane leakage and a few passages of the transition have been shown to provide cross-membrane equilibration of small polar molecules.¹⁰ This technique is particularly effective at low scanning rates where the permeability of small polar solutes becomes high without damaging the membrane¹¹ and the only effect of temperature cycling is transmembrane equilibration. We utilized this in standard protocols where the temperature of the air bath was programmed to cycle between 20 and 30 °C (which induced phase transition in all investigated membranes) at 10 °C/h for the first ~16 h of the dialysis experiment. After temperature cycling, the samples were kept isothermally at the experimental temperature for about 8 h. Then, two separate samples were retrieved with a pipet from both inside and outside the dialysis bag and diluted 5–10 times (depending on the NT concentration) in aqueous 1-propanol. The concentration of 1-propanol ranged from 25 to 75% (w/w), and it was chosen to get optimal resolution of NT and lipid in the chromatographic measurements, which used the same 1-propanol solution as eluent. All four samples (two from outside and two from inside the dialysis bag) were analyzed at least in triplicate in an Acquity UPLC instrument (Waters, Milford, MA) equipped with an evaporative light scattering (ELS) detector and an Acquity C₈ column (20 × 2.1 mm) (Waters). The trials were conducted in the isocratic mode, and the 1-propanol solution ensured dissolution of lipid and NT. This setup provided good resolution with retention times for NT and lipid of around 1.0 and 5.5 min, respectively. The concentration of lipid and NT was derived from the peak area using appropriate standard curves. As is typical for light scattering detectors, the standard curves were nonlinear. However, second-order polynomials fitted the data in all cases without systematic deviations and an average distance between measured and smoothed values of less than 0.05 mM. Therefore, the second-order polynomials were used for the quantification, and the overall error on the measured NT concentration was about ±0.1 mM.

For samples with pure DMPC, the effect of the NTs on the main phase transition was investigated by differential scanning calorimetry (DSC). To this end, equilibrated samples from the dialysis sacks were diluted 1:6 with the dialysate and loaded into the sample cell of a Nano DSC (TA Instruments, New Castle, DE) and heated from 12 to 32 °C at 0.1 °C/min and an excess pressure of 3.0 bar. The dialysate from the beaker was used in the reference cell.

Molecular dynamics simulations were performed for DPPC and the same four neurotransmitters used in the experiments (see Figure 1).

The bilayer consisted of 72 DPPC molecules (36 per leaflet), fully hydrated with 3319 water molecules (≈ 46 water molecules per lipid molecule). Each system contained one NT. The center of mass of the bilayer was located at the origin of the coordinate system ($x = y = z = 0$ Å), with z being the normal direction to the bilayer plane. Simulations were performed using the NAMD 2.5 software package¹² with the CHARMM27 force field¹³ and the TIP3P water model.¹⁴ Simulations were carried out in the *NPT* ensemble at constant pressure ($P = 1$ atm) and temperature ($T = 323$ K) using the same simulation parameters as described previously.^{15,16} To assess the statistical uncertainties in the calculated quantities, at least three independent simulations were performed for each system. Initial starting conformations of each system were generated by placing the neurotransmitter at different distances (z) from the interfacial bilayer region. Each simulation was carried out for at least 25 ns. Analyses of the trajectories were done using the VMD 1.8.7 software package.¹⁷

The choice of DMPC membranes (and DMPC mixtures) for the experiments and DPPC membranes in the simulations was based on technical restrictions. Thus, the dialysis equipment cannot operate at the higher main transition temperature of DPPC, and this hinders transmembrane equilibration of NTs by temperature cycling. For the simulations, we have used DPPC bilayers since we previously developed a consistent force field for that lipid.¹⁶ Using the original CHARMM27 parameters for phosphatidylcholine lipids, we observed that even though the temperature was above the experimental gel-to-fluid transition temperature, the bilayer had gel-phase-like properties.¹⁶ Hence, we reparametrized for DPPC based on the experimental data from Nagle and co-workers.¹⁸ In the current work, the simulations were carried out to identify possible attractive interactions and structural preferences of NT at the membrane interface. The discussion therefore assumes that these parameters are similar for DMPC and DPPC. As DMPC and DPPC have the same headgroup composition and their lateral areas in MD simulations are indistinguishable,¹⁹ it appears that this is a reasonable assumption.

Results and Data Treatment

Dialysis Measurements. The affinity of NTs for the membranes in the dialysis bag is directly reflected in the equilibrium concentrations of NT respectively inside and outside the bag. To quantify this, we first calculated the NT concentration difference, Δm_3 , in molal units:

$$\Delta m_3 = m_3^{\text{in}} - m_3^{\text{out}} \quad (1)$$

Here, and in the following, subscript 3 will identify NT, while subscripts 1 and 2 will be used for respectively water and lipid. The outside concentration, m_3^{out} , was derived directly from the raw UPLC data for the NT and an appropriate standard curve. Samples from inside the bag contained both aqueous solution and ($\sim 2\%$) lipid, and the raw UPLC data were therefore divided by the weight fraction of the aqueous part of the sample (i.e., $1 - w_2$, where w_2 is the weight fraction of the lipid). For the low concentrations of NT used here, this converted the inside concentration into molal units (i.e., moles of NT per kilogram of water). Under the definition of Δm_3 in eq 1, the quasi-ideal situation of $\Delta m_3 = 0$ corresponds to the absence of water and

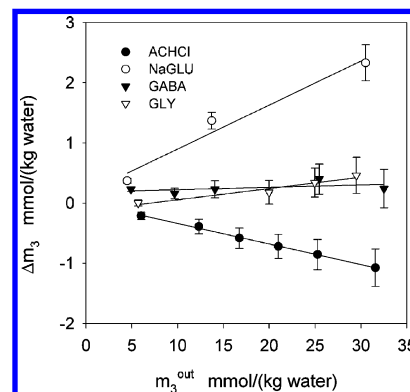


Figure 2. Examples of raw data from the dialysis equilibrium measurements expressed as Δm_3 (see eq 1) plotted against the bulk concentration of neurotransmitter, m_3^{out} . The lipid was pure DMPC at a concentration of respectively 29.3 mmol/kg of water (GABA and ACHCl experiments), 41.9 mmol/kg of water (NaGLU experiments), and 23.4 mmol/kg of water (GLY experiments). The experimental temperature was 30 °C. It appears that GLU accumulates in the dialysis bag ($\Delta m_3 > 0$), while ACH is repelled by the membranes ($\Delta m_3 < 0$). For GABA and GLY, Δm_3 is close to zero, suggesting weak interactions with pure DMPC.

NT inside the membrane and a constant NT concentration throughout the aqueous part of the membrane suspension.

Figure 2 shows examples of how Δm_3 depends on m_3^{out} for unilamellar membranes of pure DMPC.

The conventional thermodynamic approach to membrane–solute interaction is a partitioning coefficient, K , which is the equilibrium constant for the distribution of solute between the lipid and aqueous phases. In its simplest form, this may be written

$$\text{NT(aq)} \leftrightarrow \text{NT(lip)}, \quad K = \frac{m_3(\text{lip})}{m_3(\text{aq})} \quad (2)$$

where “aq” and “lip” denote the solvent (water or lipid). To relate the concentrations in eq 2 to the current measurements, we assume that the amount of NT removed from the aqueous phase (and hence, according to eq 2, partitioned into the membrane) is specified by Δm_3 . Figure 2 shows that, for NaGLU, $\Delta m_3 \sim 2.1$ mM when $m_3^{\text{out}} = 30$ mM, and the lipid concentration in this experiments was 41.9 mmol/(kg of water) (or 2.76% w/w). Hence, we get $m_3(\text{lip}) = 74$ mmol/(kg of DMPC) and $K \sim 2.5$ for sodium glutamate ($M_{\text{lipid}} = 0.678$ kg/mol). However, this approach becomes problematic for many polar solutes because their interaction with the membrane cannot be realistically described by the dissolution process which is underlying the definition of K in eq 2.²⁰ This limitation is illustrated in Figure 2, where Δm_3 for some of the systems is small or even negative. Negative Δm_3 (that is, a reduction in NT concentration inside the dialysis bag) is not compatible with the simple partitioning model inasmuch as the dissolution of any amount of NT in the membrane would increase m_3^{in} over m_3^{out} and hence give $\Delta m_3 > 0$ (a partitioning coefficient for ACHCl calculated from the data in Figure 2 would give an unphysical negative value).

We conclude that eq 2 does not provide an adequate description of the current systems and instead use the more general preferential interaction theory for the analysis. This thermodynamic approach focuses on mutual perturbations of the chemical potentials in ternary mixtures and has been extensively applied to rationalize weak protein–solute interactions on the basis of dialysis measurements (see, e.g., ref 21 and references therein). The net affinity of a solute for a

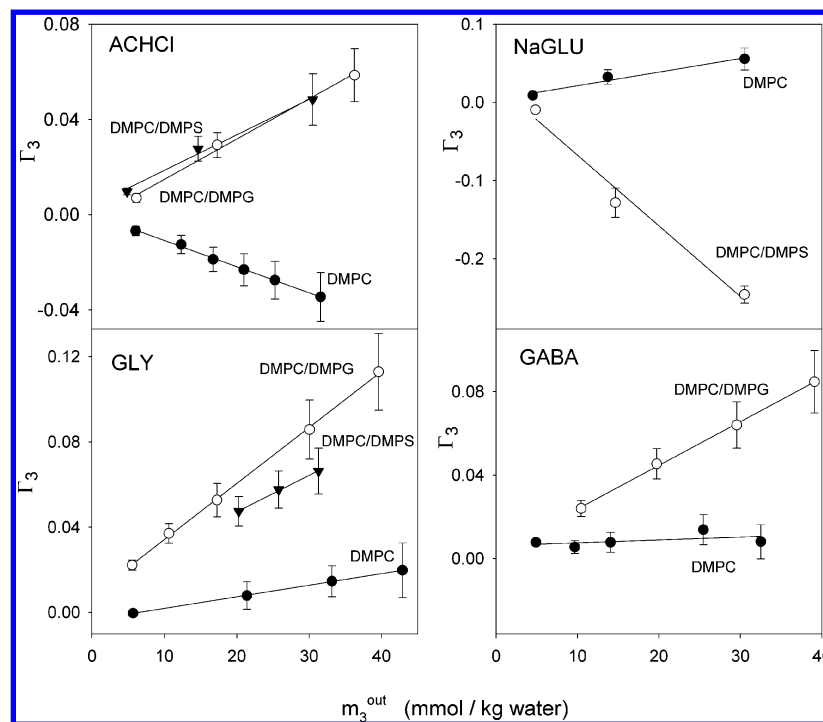


Figure 3. Net affinity at 30 °C of the investigated neurotransmitters for lipid bilayers expressed as the preferential binding parameter Γ_3 . Positive values identify favorable interactions and hence accumulation of neurotransmitter at the membrane interface. Negative values signify partial exclusion. The membranes were either pure DMPC or DMPC with 10% anionic lipid (DMPS or DMPG). The abscissa is the molal concentration of neurotransmitter.

biomolecule may be expressed by the so-called preferential binding parameter, Γ_3 .²¹

$$\Gamma_3 = -\left(\frac{\partial \mu_2}{\partial \mu_3}\right)_{P,T,m_2} = \left(\frac{\partial m_3}{\partial m_2}\right)_{\mu_3,P,T} \quad (3)$$

The first equation in eq 3 illustrates that Γ_3 reflects the mutual perturbation of the chemical potentials of lipid (μ_2) and NT (μ_3), and the second equation in eq 3 shows how Γ_3 may be derived from the equilibrium concentrations measured in a dialysis experiment (where μ_3 , P , and T are equal on the two sides of the dialysis sack). In essence, Γ_3 is a thermodynamic equivalent of a stoichiometric binding number as it quantifies the number of NT molecules which have to be added or removed to keep the chemical potential of the NT constant when one lipid molecule is added to the system. In water-rich samples (less than ~5% (w/w) lipid), Δm_3 for polar solutes has previously been shown to be essentially proportional to the lipid concentration,^{22,23} and Γ_3 may then be approximated:

$$\Gamma_3 \cong \frac{\Delta m_3}{m_2} \quad (4)$$

where m_2 is the molal concentration of lipid in the dialysis bag.

Figure 3 shows Γ_3 values calculated according to eq 4 and plotted as a function of the measured bulk concentration, m_3^{out} . Each of the four panels shows results for the interaction of one NT with both pure DMPC and some mixed membranes. Positive slopes specify attractive interactions, so-called preferential binding of NT to the bilayer. This implies that the NT–membrane interactions are more favorable than water–membrane interactions and hence that NT accumulates in the dialysis bag. Conversely, a negative slope (so-called preferential exclusion

of NT) shows that water–membrane interactions are stronger than NT–membrane interactions. The data in Figure 3 show a linear relationship and the intercept of the best fit is less than 0.01, except for NaGLU's and GLY's interactions with DMPC/DMPS. These two systems only involved three data points, and we conclude that, to within the experimental precision, Γ_3 in Figure 3 is proportional to m_3^{out} .

To further interpret the thermodynamic information in Figure 3, we applied the so-called “two-domain model”.^{24,25} The basic premise of this approach is the separation of the aqueous phase into respectively the bulk and a local domain near the membrane interface. Each of the two domains is assigned a distinct NT concentration. The local (interfacial) domain is specified by a number of NT molecules (B_3) and water molecules (B_1) per lipid molecule and these values are related to Γ_3 :^{24,25}

$$\Gamma_3 = B_3 - B_1 \frac{m_3^{\text{out}}}{m_1} \quad (5)$$

where m_1 is the number of moles in 1 kg of pure water (55.6 mol). The distribution of NT between the interfacial domain and the bulk may then be expressed as a partitioning coefficient, P , defined in the first equation of eq 6. If we insert eq 5 in this definition, P may be expressed as a function of the measured Γ_3 :

$$P \equiv \frac{m_3^{\text{interface}}}{m_3^{\text{bulk}}} \approx \frac{\Gamma_3 [55.6 \text{ mol (kg of water)}^{-1}]}{m_3^{\text{out}} B_1} + 1 \quad (6)$$

Values of P can be calculated from eq 6 if an (extra-thermodynamic) choice of B_1 (i.e., the extent of the local

TABLE 1: Net Affinity of Neurotransmitters for Different Bilayers at 30 °C^a

lipid	NT	slope ($\Gamma_3/m_3^{\text{out}}$)	<i>P</i>
DMPC	ACHCl	-1.10 ± 0.03	—
	NaGLU	1.74 ± 0.31	5.8
	GLY	0.54 ± 0.06	2.5
DMPC–DMPG	GABA	0.14 ± 0.14	1.4
	ACHCl	1.70 ± 0.12	5.7
	GLY	2.63 ± 0.04	8.3
DMPC–DMPS	GABA	2.09 ± 0.05	6.8
	ACHCl	1.49 ± 0.14	5.1
	NaGLU	-9.05 ± 1.25	—
	GLY	1.72 ± 0.08	5.8

^a The slopes (in kg of water/mol of NT) are from linear fits to the data in Figure 3, and the *P* values are calculated from these slopes using eq 6.

domain) is made. We chose $B_1 = 20$ since the physical properties of lipid membranes normally attain values characteristic of full hydration when the water content is about 20–30 H₂O (lipid)^{−1}.²⁶ To put this number into perspective, we note that the projected lateral area of a DMPC membrane at 30 °C is about 60 Å² per lipid²⁷ and that the (corrugated) water accessible area is approximately twice this value.²⁸ As one water molecule covers an area of about 9 Å²,²⁹ it follows that the local domain defined as $B_1 = 20$ corresponds to about two to three water layers.

Since the current work is in the millimolar concentration range, we assume that $B_1 = 20$ for all NT concentrations (this implies that the amount of NT entering the hydration zone is too small to displace significant amounts of water). Insertion of this B_1 value and Γ_3 data determined for pure DMPC (Figure 3) in eq 5 shows that *P* is about 6 for NaGLU and 3 for GLY. For GABA–DMPC, the slope in Figure 3 is indistinguishable from the experimental scatter, suggesting an even distribution of this NT between the two domains ($P \sim 1$). Finally, the negative slope for ACHCl–DMPC translates to a *P* value below 0 for the current choice of B_1 . This implies that the affinity of DMPC for water is much higher than for ACHCl and thus that the (average) depletion zone for ACHCl comprises more than 20 water molecules per lipid.

Incorporation of 10% anionic lipid (DMPG or DMPS) strongly modulates the membrane affinity of the investigated NTs. The two uncharged molecules (glycine and GABA) show severalfold increase in Γ_3 , and values of *P* derived from eq 6 are about 7 for GABA and 6–8 for glycine. The NT salts respond to the incorporation of anionic lipid in accord with the charge of the NT. Thus DMPS or DMPG generates a strong increase in the affinity of ACHCl and a pronounced repulsion of NaGLU. This shows that the affinity of these ion pairs is mainly governed by the ionic NT and not the Cl[−] or Na⁺ counterions. Table 1 provides an overview of the strength of NT–membrane interaction derived from Figure 3. As all Γ_3 values are essentially proportional to m_3^{out} , the net interaction strength can be expressed as the slope $\Gamma_3/m_3^{\text{out}}$ or the associated *P* coefficient defined in eq 6.

Relationships of lipid phase behavior and the affinity of the NT were tested with mixed DPPC/DLPC (1:1). This model membrane was chosen because its phase diagram is well described and shows a gel–fluid coexistence region from about 0 to 30 °C at this composition.³⁰ Figure 4 shows the temperature dependence of Γ_3 for the interaction of respectively ACHCl, NaGLU, and GLY and this lipid mixture. The vertical dashed line in Figure 4 represents the phase boundary above which the membrane is in the fluid phase. The picture of preferential

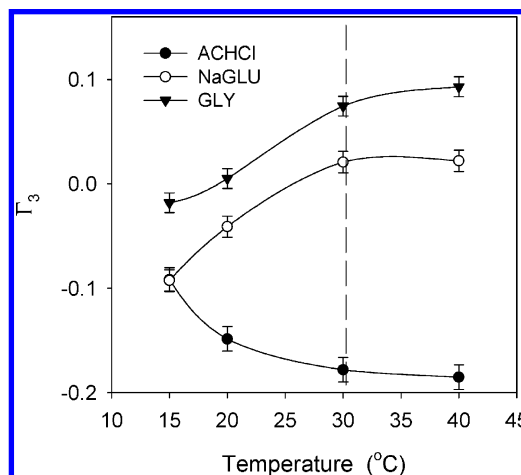


Figure 4. Temperature dependence of the preferential binding parameter, Γ_3 , for the interaction of DPPC/DLPC and three neurotransmitters. The concentration, m_3^{out} , is 30, 27, and 25 mmol/kg of water for respectively ACHCl, NaGLU, and GLY. The dashed line shows the phase boundary between the gel–liquid coexistence region and the liquid phase.

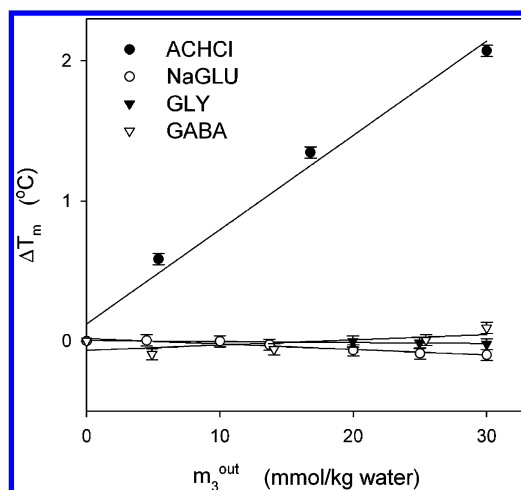


Figure 5. Dependence of the main phase transition temperature (T_m) for DMPC on the concentration of neurotransmitters. The transition in pure buffer was at 23.9 °C, and the ordinate shows the change ΔT_m induced by NT in the solvent.

exclusion of ACHCl and attraction of GLY observed for DMPC (Figure 3) reoccurs in the results for this PC mixture, although the interaction with glycine is somewhat stronger (corresponding to $P \sim 11$ at 40 °C) than for membranes of pure DMPC. All three curves change monotonically with temperature and thus do not suggest any particular affinity for the phase coexistence region.

Calorimetry. The effect of the four NTs in the millimolar concentration range on the phase behavior of pure DMPC is illustrated in Figure 5. It appears that ACHCl strongly increases T_m (the slope in Figure 5 is 67 ± 6 (SE) °C/(mol/kg of water)). NaGLU generates a small negative change in T_m (-4 ± 0.5 °C/(mol/kg of water) and the other NTs exert still smaller effects, which are comparable to the experimental scatter. Comparison to Figure 3 shows that NT-induced changes in T_m and Γ_3 are in general inversely related. Thus, NTs that induce positive changes in Γ_3 decrease T_m and vice versa. GABA leaves both Γ_3 and T_m essentially unchanged.

MD Simulations. Figure 6 shows the probability distributions of the center of mass of the different NTs (black line) and the phosphorus atom of the lipid (green line; P_{bilayer}). It appears that

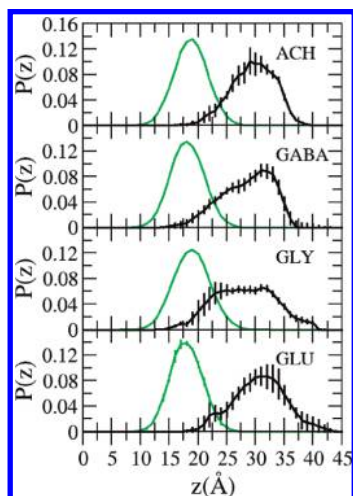


Figure 6. Probability of respectively the phosphorus atom in DPPC (green line) and center of mass of the different neurotransmitters (black line; NTs indicated in the figure) as a function of the distance from the center of mass of the lipid bilayer. Error bars are based on at least three independent simulations.

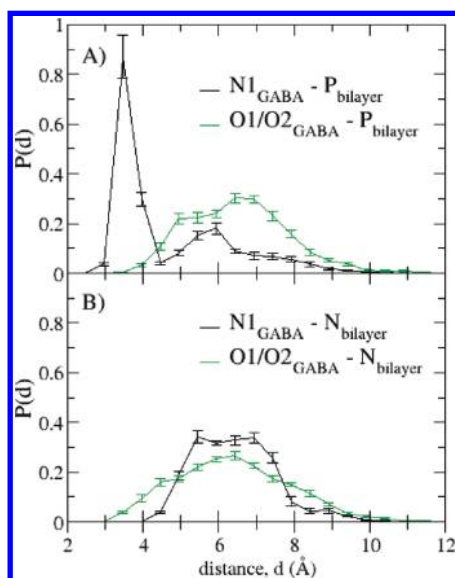


Figure 7. Probability of electrostatic contacts between GABA and DPPC. Probability distribution of distances between polar atoms of the neurotransmitter (N1 or the carboxylate oxygen O1/O2; see Figure 1) and (A) the phosphorus atoms in the phosphate group of the lipid or (B) the nitrogen atom in the choline groups of the lipid. Error bars are based on at least three independent simulations.

all NTs show a broad distribution with some occupancy in the membrane interface (overlapping the outer part of the P_{bilayer} distribution), but no penetration into the membrane core. This observation supports the validity of the interfacial approach used for the analysis of the experimental data.

One purpose of the MD study was to identify possible modes of interaction that could account for the measured affinities. To this end, we assessed the frequency of intermolecular contact between charged groups on respectively membrane and NT. In this analysis, we considered only “interfacial” NT molecules, which were operationally defined as those for which the center of masses were located at $z < 22$ Å. We then recorded the distances from the polar atoms (N or O) in NTs to charged groups in the lipid (phosphate or choline) and plotted the distribution probabilities as exemplified for GABA in Figure 7.

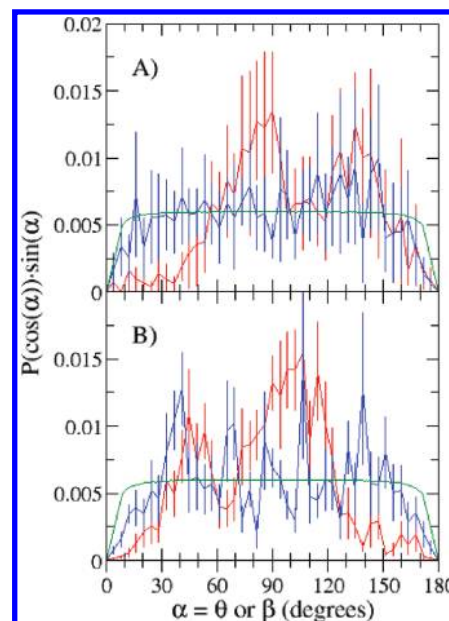


Figure 8. Probability functions of $\cos(\theta)$ (red) and $\cos(\beta)$ (blue) for GABA and GLY. For comparison, the distribution function for the free rotation of the angle is shown in dark green. Vertical lines show the standard deviation, SD, based on at least three independent simulations.

The distinct peak in Figure 7A with a maximum at 3.5 Å specifies a salt bridge between the nitrogen atom of GABA (N1; Figure 1) and the phosphate group of DPPC. The opposite electrostatic interaction (lipid nitrogen and neurotransmitter oxygen, Figure 7B) shows a broad peak with a maximum value at ~ 6.5 Å, which is ~ 3 times lower than observed for the $N1_{\text{GABA}}-P_{\text{bilayer}}$ interactions. In fact, the probability distribution for this contact is similar to the one found for repulsive ionic interactions (e.g., the $O_{\text{GABA}}-P_{\text{bilayer}}$ interaction in Figure 7B), and we conclude that the contact of neurotransmitter oxygen and lipid nitrogen is not essential for the membrane–NT affinity. Results for glycine (not shown) were very similar to those for GABA with a strong $N_{\text{NT}}-P_{\text{bilayer}}$ peak at 3.5 Å. Data for ACH did not identify any strong interactions, and this along with the low concentration of ACH in the interfacial layer (Figure 6) is in line with the negative experimental values of Γ_3 (Figure 3). Glutamate, with two negative charges and one positive charge, allows for additional electrostatic interactions. However, the role of the positively charged group (N6; Figure 1) in the NT–bilayer interactions is significantly reduced by the neighboring carboxylate group (O1/O2; Figure 1). The effective positive charge is reduced and no NT–lipid salt bridges are observed (data not shown).

Dominant positions and orientations of interfacial GABA and glycine molecules were investigated through the angles θ and β defined in Figure 1. θ is the angle between the $N_{\text{NT}}-P_{\text{bilayer}}$ minimal distance vector (i.e., the strong salt bridge) and the membrane normal (the z -axis), and it illustrates how deeply the NT molecules penetrate into the membrane. Thus, if $\theta = 90^\circ$ the N_{NT} and P_{bilayer} atoms will be at the same depth (z -value) while smaller (larger) θ implies that N_{NT} is above (below) P_{bilayer} . β is the angle between the head–tail distance vector of the NT and the membrane normal, and hence the angle illustrates the tilt of the interfacial NT molecules. If β is around 90° , the NT is aligned along the membrane interface, while values far from 90° (i.e., near 0° or 180°) correspond to an intercalated position where the NT aligns with the lipid chains.

The results in Figure 8 show wide probability distributions of respectively θ and β that are expected for a weak interaction.

However, it appears that θ (red) for both neurotransmitters shows a maximum near 90° indicative of N_{NT} being at the same depth as $P_{bilayer}$. For GABA a secondary maximum around 140° suggests another favorable position deeper (i.e., below $P_{bilayer}$) in the membrane. The probability distribution of β (blue) extracted from the GABA simulations resembles the distribution of free rotation (green), and interfacial GABA molecules do not show preference for particular orientations with respect to the lipid plane (e.g., parallel or orthogonal). GLY penetrates more into the interfacial membrane region than GABA (Figure 6), and the probability distribution of β shows some weak maxima (e.g., around at 40° and 140°) corresponding to orientations where the head–tail direction of the NT is tilted 45° with respect to the membrane plane. The statistical uncertainties in this analysis are relatively high, and hence structural preferences of NT at the membrane interface appear to be quite weak.

The operational cutoff for interfacial NTs ($z < 22 \text{ \AA}$) may also be used to assess the net affinity as reflected by the simulations. To this end, we enumerated interfacial and bulk NT by integration of the probability functions in Figure 6 (respectively above and below $z = 22 \text{ \AA}$). The two NT concentrations (local for $z < 22 \text{ \AA}$ and bulk for $z > 22 \text{ \AA}$) were then calculated and inserted in eq 6 to get the partitioning coefficient, P . The P values derived from this analysis were consistently less than unity (corresponding to preferential exclusion) and hence the simulations gave an overall picture of weaker membrane–NT interactions than the experiments. However, it is well established that free energies of interactions (or partitioning coefficients) cannot be readily derived from standard MD simulations, and commonly umbrella sampling or steered molecular dynamics simulations are applied to assess free energies.^{31–35} We will therefore refrain from further analysis of this parameter until such analysis becomes available for NT–membrane systems and focus on the analysis of local structures in the MD data.

Discussion

Dialysis equilibrium measurements provide a general and model-independent picture of the strength of solute–biopolymer interactions, and we have applied this to elucidate the net affinity of four polar NTs for lipid bilayer membranes of different compositions. This type of information is essential in discussions of nonsaturable NT interactions in synaptic nerve transmission and a possible role of NTs as “endogenous anesthetics”.⁴

Results in Figure 3 suggest that the charge of the NT is a main determinant of its affinity for pure DMPC bilayers. Thus, ACHCl (with the cationic ACH) exhibits preferential exclusion from the membrane interface ($\Gamma_3 < 0$), while NaGLU (with anionic GLU) is preferentially bound ($\Gamma_3 > 0$). We note that the Γ_3 data for these two (charged) NTs pertain to the average affinity of the components in the investigated ion pairs (i.e., $[\text{Na}^+, \text{GLU}^-]$ and $[\text{ACH}^+, \text{Cl}^-]$). The two neutral (zwitterionic) NTs GLY and GABA fall between these extremes and show weak interactions with membranes of pure DMPC. The increase of Γ_3 with NT concentration is more pronounced for GLY than for GABA, implying that GLY associates with the membrane surface more than GABA. Comparison of these dialysis results for pure DMPC and the DSC data in Figure 5 shows that for a given NT the slopes of respectively Γ_3 (Figure 3) and T_m (Figure 5) have opposite signs (and for GABA the slopes are ~ 0 for both parameters). This behavior suggests that changes in T_m are governed by solute-induced perturbations of the interfacial free energy^{36–39} rather than a freezing point depression as seen

for more hydrophobic solutes that preferentially dissolve in the fluid phase.^{40,41} Hence, dialysis and DSC measurements are mutually consistent and the results support the choice of an interfacial model for the interaction (cf. eq 6). Interpretation of the results for pure DMPC along the lines of the two-domain model shows that effects for the charged NTs are quite significant. The preferential exclusion of ACHCl corresponds to its (average) absence from several water layers at the membrane interface, and the attractive interactions of NaGLU suggest that the NT:water molar ratio in the hydration zone is 6-fold increased with respect to the bulk (Table 1). The systematic relationship between the charge of the NT and its affinity for pure DMPC points toward a dominant electrostatic component of the interaction. The MD simulations suggested that this was the attraction of $-\text{NH}_3^+$ (on the NT) and lipid $-\text{PO}_4^-$, while the bulkier $-\text{N}(\text{CH}_3)_3^+$ group on either ACH or lipid was unable to make strong interactions. In addition, it is also likely that the affinity of the NTs will be influenced by the very strong dipole potential at the membrane interface, which is positive toward the inner part of the headgroup region⁴² and has been associated with the binding of hydrophobic and possibly also small anions to the membrane interface.⁴³

To elucidate the role of Coulombic effects further, we tested the affinity of the NTs for DMPC membranes doped with 10% anionic lipid (either DMPS or DMPG). Three main observations were made in these experiments. (i) The affinity of the two NT salts was changed dramatically by the anionic lipids. Thus, ACHCl was preferentially bound to the mixed, anionic membranes while NaGLU was preferentially excluded (Figure 3). (ii) We did not detect sizable differences in NT affinity for membranes containing either PG or PS. (iii) Introduction of the anionic lipids strongly increased the membrane's affinity for the zwitterionic NTs GLY and GABA. Observation (i) supports the above suggestion that the NT (rather than the counterion) governs Γ_3 for the ion pairs ACHCl and NaGLU. With respect to (ii), we note that PS is commonly found in high concentrations in the synaptic membrane while PG is not.^{44,45} In fact, membranes with a high content of PC and 10–15% PS (i.e., similar to the DMPC/DMPS membranes studied here) are commonly found in some synapses.⁴⁶ However, the similarity of the results for DMPG and DMPS observed here speaks against any particular role of PS in the binding of NT and rather points toward the surface charge per se as an important factor. The result with the most direct pertinence to the hypothesis of Cantor discussed in the Introduction is probably (iii), which underscores that NTs may indeed exhibit a pronounced interaction with lipid bilayers. Thus, if the affinity of GLY or GABA (Figure 3) for mixed DMPC/DMPG membranes is compared to well-studied solutes such as the normal alcohols, we find that it falls between the affinities (for pure PC) of 1-pentanol and 1-butanol.^{47–49} This similarity only regards the overall strength—not the mode—of interaction. The different modes of interaction may be illustrated by the influence of hydrophobic moieties. For alcohols, the affinity for membranes systematically increases with the size of the hydrophobic chain (K as defined in eq 2 increases ~ 2.5 -fold for each additional methylene group in normal alcohols^{20,50}). Conversely, comparison of GLY and GABA, which have the same architecture of functional groups but different hydrophobic chains, suggests that hydrophobic interactions are of little importance for these NTs. In fact, the less hydrophobic molecule (GLY) consistently interacts more strongly with the membranes. The overall picture of NT–membrane interaction obtained here is therefore that they are specific in the sense that moderate changes in the molecular structure

of the NT and/or the composition of the membrane strongly modifies the interaction strength. However, they are structurally unspecific inasmuch as no particular preference in the organization of NT on the membrane surface could be identified from the MD data. The specificity in interaction strength suggests that bilayer-mediated modification of membrane proteins could be particular for a certain agent or membrane type.

In conclusion, we have found that interactions of NT and lipid bilayers show a remarkable variation with the chemical structure of the NT and the composition of the membrane. This picture is very different from the systematic structure–affinity relationship found for the partitioning of amphiphilic solutes such as alcohols or carboxylic acids,^{3,51} and it suggests that Coulombic forces and specific polar interactions give rise to attractive and repulsive contributions that govern the NT interactions. The MD simulations suggested that the interaction of the neurotransmitter's nitrogen atom and the lipid phosphate group was essential for the net affinity. For bilayers with 10% anionic lipid and for (uncharged) 1:1 mixtures of DPPC and DLPC, we found examples of quite strong interactions, which were comparable in strength with those typically found for medium-sized alcohols such as butanol and pentanol. For pure DMPC membranes the interactions were typically severalfold weaker. The occurrence of significant membrane interactions for polar nonelectrolytes such as GLY and GABA is unusual and appears to be a necessary criterion for Cantor's hypothesis. Clearly, it is far from a sufficient criterion, and future studies of the effects of such interactions on the properties and dimensions of the bilayer and its coupling to protein function are required to further develop the theory. It is our hope that the fundamental elucidation of interaction strengths can provide some guidance for these studies.

Acknowledgment. This work was supported by grants from the Lundbeck Foundation, the Danish Research Agency (Grant 272-06-0505), and the Danish National Research Foundation through the establishment of MEMPHYS, Center for Biomembrane Physics.

References and Notes

- (1) Gilles, R. *Comp. Biochem. Physiol., Part A: Physiol.* **1997**, *117*, 279.
- (2) Hodgkin, A. L.; Horowicz, P. *J. Physiol. (London)* **1960**, *153*, 404.
- (3) Janoff, A. S.; Miller, K. W. *Biol. Membr.* **1982**, *4*, 417.
- (4) Cantor, R. S. *Biochemistry* **2003**, *42*, 11891.
- (5) Sonner, J. M. *Anesth. Analg.* **2008**, *107*, 849.
- (6) Milutinovic, P. S.; Yang, L.; Cantor, R. S.; Eger, E. I.; Sonner, J. M. *Anesth. Analg.* **2007**, *105*, 386.
- (7) Rolandi, R.; Robello, M.; Mao, C.; Mainardi, P.; Besio, G. *Cell Biophys.* **1990**, *16*, 71.
- (8) Pico, C.; Pons, A.; Palou, A. *Biosci. Rep.* **1991**, *11*, 223.
- (9) Pico, C.; Pons, A.; Palou, A. *Int. J. Biochem. Cell Biol.* **1995**, *27*, 761.
- (10) Crowe, L. M.; Crowe, J. H. *Biochim. Biophys. Acta* **1991**, *1064*, 267.
- (11) Hays, L. M.; Crowe, J. H.; Wolkers, W.; Rudenko, S. *Cryobiology* **2001**, *42*, 88.
- (12) Phillips, J. C.; Braun, R.; Wang, W.; Gumbart, J.; Tajkhorshid, E.; Villa, E.; Chipot, C.; Skeel, R. D.; Kale, L.; Schulten, K. *J. Comput. Chem.* **2005**, *26*, 1781.
- (13) MacKerell, A. D.; Bashford, D.; Bellott, M.; Dunbrack, R. L.; Evanseck, J. D.; Field, M. J.; Fischer, S.; Gao, J.; Guo, H.; Ha, S.; Joseph-McCarthy, D.; Kuchnir, L.; Kucera, K.; Lau, F. T. K.; Mattos, C.; Michnick, S.; Ngo, T.; Nguyen, D. T.; Prodhom, B.; Reiher, W. E.; Roux, B.; Schlenkerich, M.; Smith, J. C.; Stote, R.; Straub, J.; Watanabe, M.; Wiorkiewicz-Kuczera, J.; Yin, D.; Karplus, M. *J. Phys. Chem. B* **1998**, *102*, 3586.
- (14) Guenet, J.; Kollman, P. A. *J. Comput. Chem.* **1993**, *14*, 295.
- (15) Peters, G. H.; Hansen, F. Y.; Moller, M. S.; Westh, P. *J. Phys. Chem. B* **2009**, *113*, 92.
- (16) Sonner, J.; Jensen, M. O.; Hansen, F. Y.; Hemmingsen, L.; Peters, G. H. *Biophys. J.* **2007**, *92*, 4157.
- (17) Humphrey, W.; Dalke, A.; Schulten, K. *J. Mol. Graphics* **1996**, *14*, 33.
- (18) Nagle, J. F.; Zhang, R. T.; Tristram-Nagle, S.; Sun, W. J.; Petrache, H. L.; Suter, R. M. *Biophys. J.* **1996**, *70*, 1419.
- (19) Kupiainen, M.; Falck, E.; Ollila, S.; Niemela, P.; Gurtovenko, A. A.; Hyvonen, M. T.; Patra, M.; Karttunen, M.; Vattulainen, I. *J. Comput. Theor. Nanosci.* **2005**, *2*, 401.
- (20) Westh, P. *Soft Matter* **2009**, *5*, 3249.
- (21) Timasheff, S. N. *Adv. Protein Chem.* **1998**, *51*, 355.
- (22) Westh, P. *Biophys. J.* **2003**, *84*, 341.
- (23) Westh, P. *Biochim. Biophys. Acta, Biomembr.* **2004**, *1664*, 217.
- (24) Felitsky, D. J.; Record, M. T. *Biochemistry* **2004**, *43*, 9276.
- (25) Record, M. T.; Zhang, W. T.; Anderson, C. F. *Adv. Protein Chem.* **1998**, *51*, 281.
- (26) Koynova, R.; Caffrey, M. *Biochim. Biophys. Acta, Rev. Biomembr.* **1998**, *1376*, 91.
- (27) Nagle, J. F.; Tristram-Nagle, S. *Biochim. Biophys. Acta, Rev. Biomembr.* **2000**, *1469*, 159.
- (28) Tuchsien, E.; Jensen, M. O.; Westh, P. *Chem. Phys. Lipids* **2003**, *123*, 107.
- (29) Gill, S. J.; Dec, S. F.; Olofsson, G.; Wadso, I. *J. Phys. Chem.* **1985**, *89*, 3758.
- (30) Seeger, H. M.; Fidorra, M.; Heimburg, T. *Macromol. Symp.* **2004**, *219*, 85.
- (31) MacCallum, J. L.; Bennett, W. F. D.; Tieleman, D. P. *Biophys. J.* **2008**, *94*, 3393.
- (32) Johansson, A. C. V.; Lindahl, E. *Proteins* **2008**, *70*, 1332.
- (33) Allen, T. W.; Andersen, O. S.; Roux, B. *Biophys. J.* **2006**, *90*, 3447.
- (34) Beckstein, O.; Tai, K.; Sansom, M. S. P. *J. Am. Chem. Soc.* **2004**, *126*, 14694.
- (35) Zhu, F. Q.; Tajkhorshid, E.; Schulten, K. *Biophys. J.* **2002**, *83*, 154.
- (36) Cevc, G. *Ber. Bunsen-Ges. Phys. Chem. Chem. Phys.* **1988**, *92*, 953.
- (37) Koynova, R.; Brankov, J.; Tenchov, B. *Eur. Biophys. J. Biophys. Lett.* **1997**, *25*, 261.
- (38) Westh, P. *Phys. Chem. Chem. Phys.* **2008**, *10*, 4110.
- (39) Westh, P.; Peters, G. H. Organic and Inorganic Osmolytes at Lipid Membrane Interfaces. In *Structure and Dynamics of Membranous Interfaces*; Nag, K., Ed.; John Wiley & Sons, Inc.: New York, 2008; p 227.
- (40) Heimburg, T. *Thermal Biophysics of Membranes*; Wiley-VCH: Weinheim, 2007.
- (41) Tamura, K.; Kaminoh, Y.; Kamaya, H.; Ueda, I. *Biochim. Biophys. Acta* **1991**, *1066*, 219.
- (42) Starke-Peterkovic, T.; Clarke, R. J. *Eur. Biophys. J. Biophys. Lett.* **2009**, *39*, 103.
- (43) Flewelling, R. F.; Hubbell, W. L. *Biophys. J.* **1986**, *49*, 541.
- (44) Cotman, C.; Blank, M. L.; Moehl, A.; Snyder, F. *Biochemistry* **1969**, *8*, 4606.
- (45) Hitzemann, R. J.; Johnson, D. A. *Neurochem. Res.* **1983**, *8*, 121.
- (46) Rotstein, N. P.; Arias, H. R.; Barrantes, F. J.; Avelldano, M. I. *J. Neurochem.* **1987**, *49*, 1333.
- (47) Katz, Y.; Diamond, J. M. *J. Membr. Biol.* **1974**, *17*, 101.
- (48) Westh, P.; Trandum, C.; Koga, Y. *Biophys. Chem.* **2001**, *89*, 53.
- (49) Zhang, F. L.; Rowe, E. S. *Biochemistry* **1992**, *31*, 2005.
- (50) Janoff, A. S.; Pringle, M. J.; Miller, K. W. *Biochim. Biophys. Acta* **1981**, *649*, 125.
- (51) Hoyrup, P.; Davidsen, J.; Jorgensen, K. *J. Phys. Chem. B* **2001**, *105*, 2649.